Electronic Supplementary Material (ESI) for RSC Advances.

Enhancement of photocatalytic efficacy exploiting copper doping in nano-hydroxyapatite for degradation of Congo Red dye

Md. Sahadat Hossain, Supanna Malek Tuntun, Newaz Mohammed Bahadur and Samina Ahmed

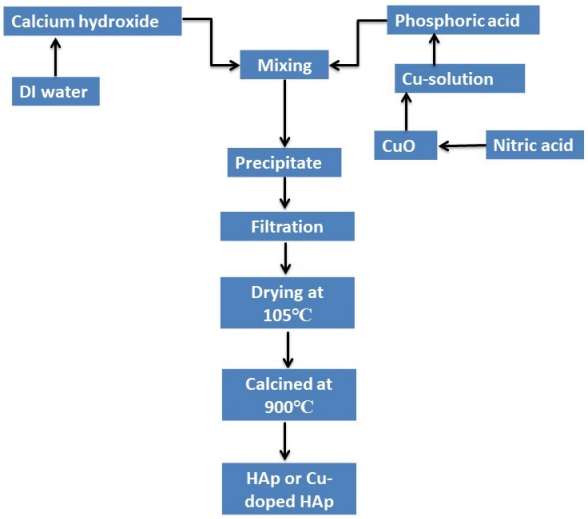

Scheme S_1: Preparation process of HAp and Cu-doped HAp

2.4. Adsorption study

For the assessment of adsorption activity of synthesized samples, 20 ppm of dye solution was prepared using solid dye and DI water, and the experiment was performed under dark condition following a methodology as described in the respective section. The removal percentage (R_p) of samples was computed utilizing the following equation (Eq. 13), where C_o and C_t represent the initial and final (at time "t") concentration, respectively[1]. The adsorption capacity (q_e) of the adsorbent was enumerated with the aid of equation 14, where W and V denote the weight of the adsorbent and the volume of the aqueous solution of adsorbate, respectively[2,3]. The removal percentage and adsorption capacity were calculated in percentage and mg/g basis, respectively.

Crystallite size calculation using various models

Liner straight-line method of Scherrer's equation

Determination of crystallite size of crystalline materials is very important for any precise characterization and applications. Thus, crystallite sizes of synthesized HAp samples were calculated by using different model equations. D_L (crystallite size from the liner straight-line method of Scherrer's equation) was calculated from the modified form of Scherrer's equation, known as the liner straight-line method of Scherrer's equation is given as follows,

$$\cos\theta = \frac{K\lambda}{Dc} \times \frac{1}{\beta} = \frac{K\lambda}{DL} \times \frac{1}{\beta} \quad (1)$$

Equation 1 was compared with the liner straight line equation as below,

$$y = mx + c \quad (2)$$

A graphical scheme was prepared by using equation 1 where cos θ (in degree) was plotted in the y-axis and $\frac{1}{\beta}$ (in radian) in the x-axis. Fig 1 shows the prepared graphs for the samples. The slope m = $\frac{K\lambda}{DL}$ was obtained by comparing equation 1 & 2 which was used to calculate the crystallite size, D_L. Because of the too large crystallite size, this method is invalid for synthesized HAp samples.

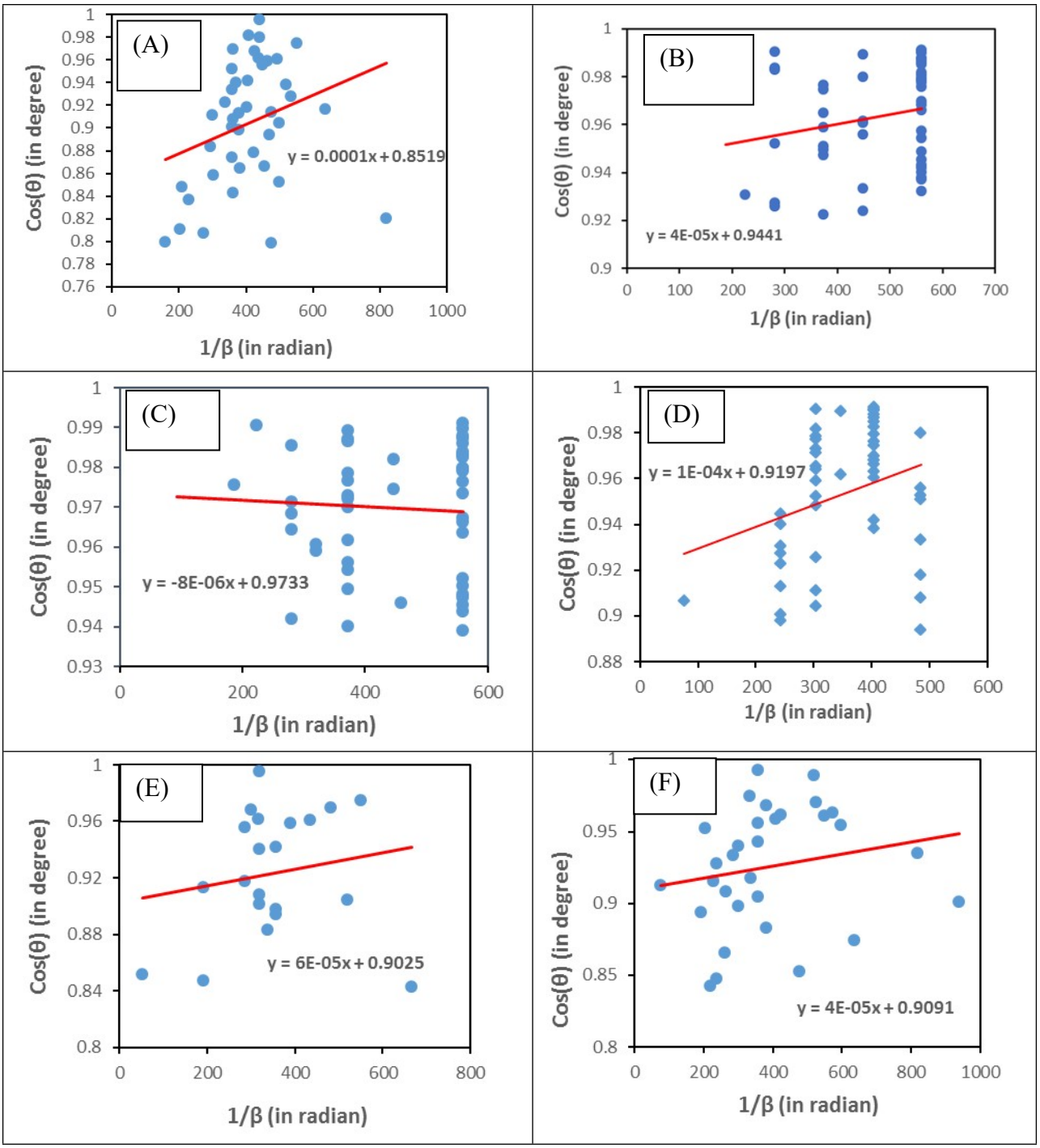

Figure S_1: Graphical representation of crystallite size for **(A)** HAp, (**B)** 0.32 Cu HAp, (**C)** 0.63 Cu HAp, (**D)** 1.25 Cu HAp, (**E)** 2.5 Cu HAp, (**F)** 5 Cu HAp using liner straight line method of Scherrer's equation.

Monshi- Scherrer method

The crystallite size of synthesized HAps was also calculated by using the Monshi-Scherrer method or modified Scherrer formula (equation 3) where the

crystallite size was represented by D_M. The equation was formed by rearranging and taking 'ln' in Scherrer's equation which is as follows,

Monshi-Scherrer method, $\ln \beta = \ln \frac{1}{\cos\theta} + \ln \frac{K\lambda}{DM}$ (3)

From equation 3, ln β (in radian) was plotted in the y-axis and $\ln \frac{1}{\cos\theta}$ (in degree) in the x-axis. The obtained graphs are included in Fig. 2. Equation 2 & 3 were compared and written as below,

$\ln \frac{K\lambda}{DM}$ = intercept (4)

or, $\frac{K\lambda}{D_M} = e^{(intercept)}$ (5)

The crystallite sizes (D_M) were calculated by taking intercepts using equation 3. The resultant values were identical to the values calculated by using Scherrer's formula. So it can be presumed that Monshi-Scherrer method is valid for synthesized HAp samples.

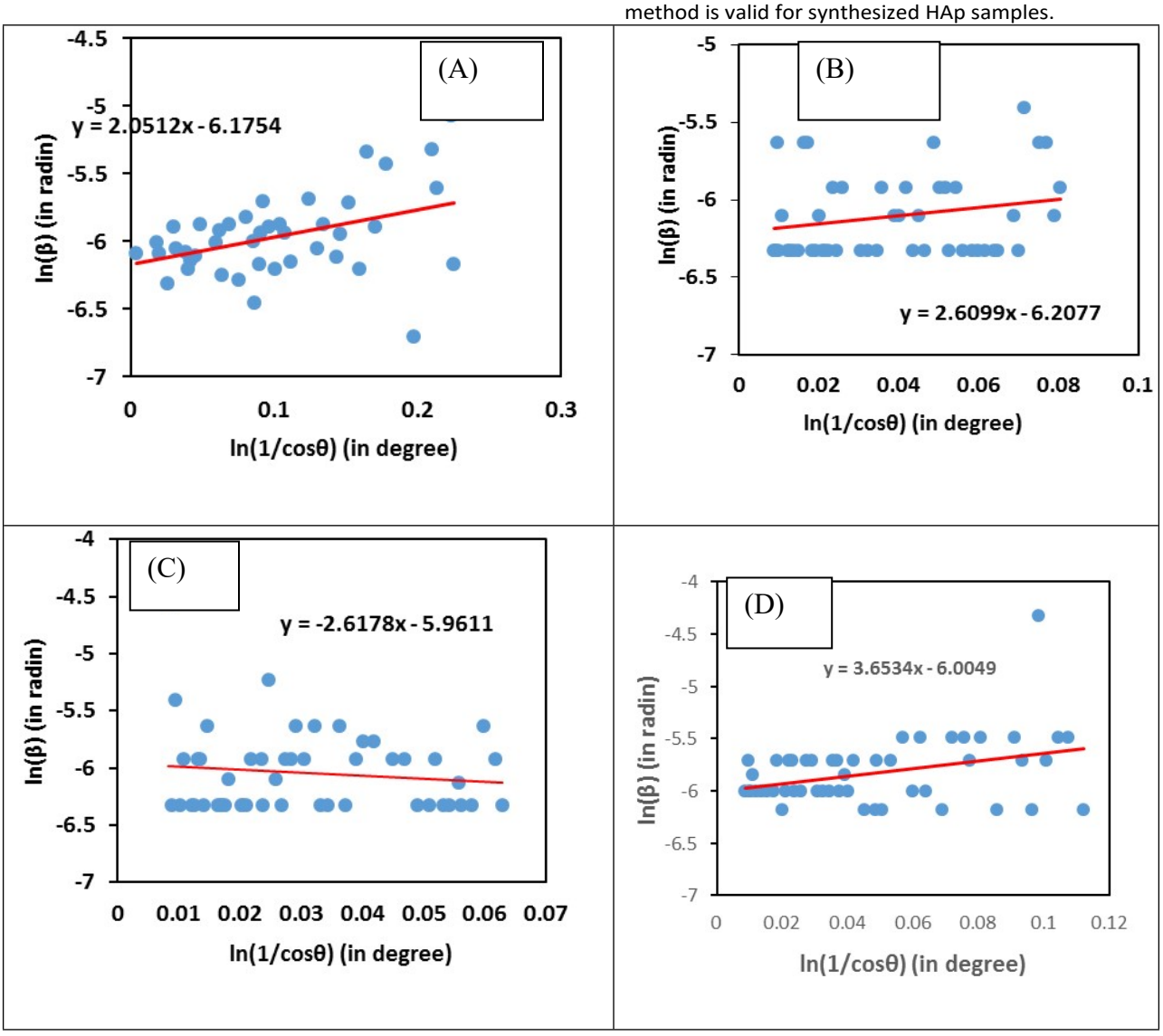

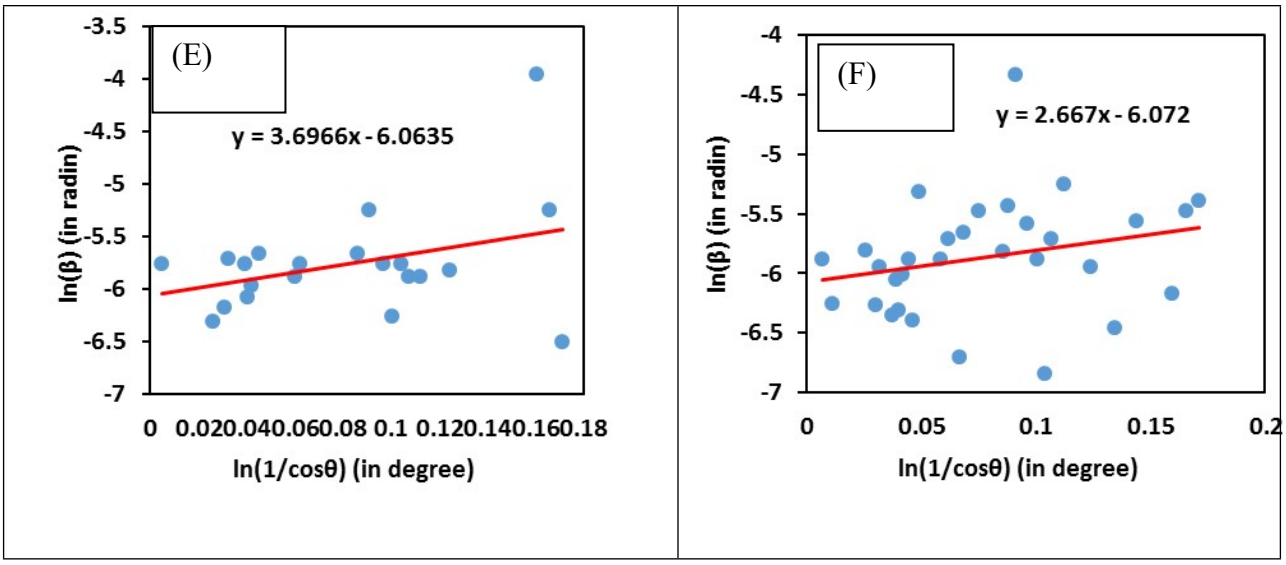

Figure S_2: Graphical representation of crystallite size for **(A)** HAp, (**B)** 0.32 Cu HAp, (**C)** 0.63 Cu HAp, (**D)** 1.25 Cu HAp, (**E)** 2.5 Cu HAp, (**F)** 5 Cu HAp using Monshi-Scherrer method.

Williamson-Hall method

To calculate the crystallite size which is very important for nanocrystals through the grain boundaries, point defects, dislocation and stacking, the William-Hall method is the best choice. The equation is given below.

$$\beta_{total} \cos\theta = \frac{K_B\lambda}{D_W} + 4\varepsilon \sin\theta \quad (6)$$

Fig. 3 was obtained by plotting 4 sin θ (in degree) and β_{total} cos θ (in radian, degree) in the x-axis and y-axis respectively. Equation 6 and 2 were compared and the intercept, y was computed from the graphs equal to the value $\frac{K_B\lambda}{D_W}$, which was applied to calculate the crystallite sizes of the synthesized samples.

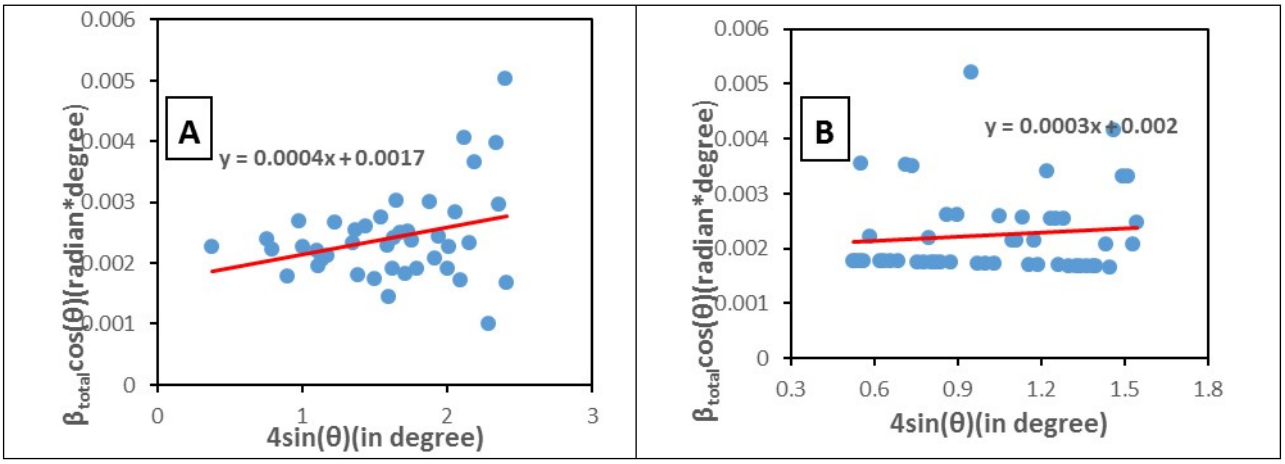

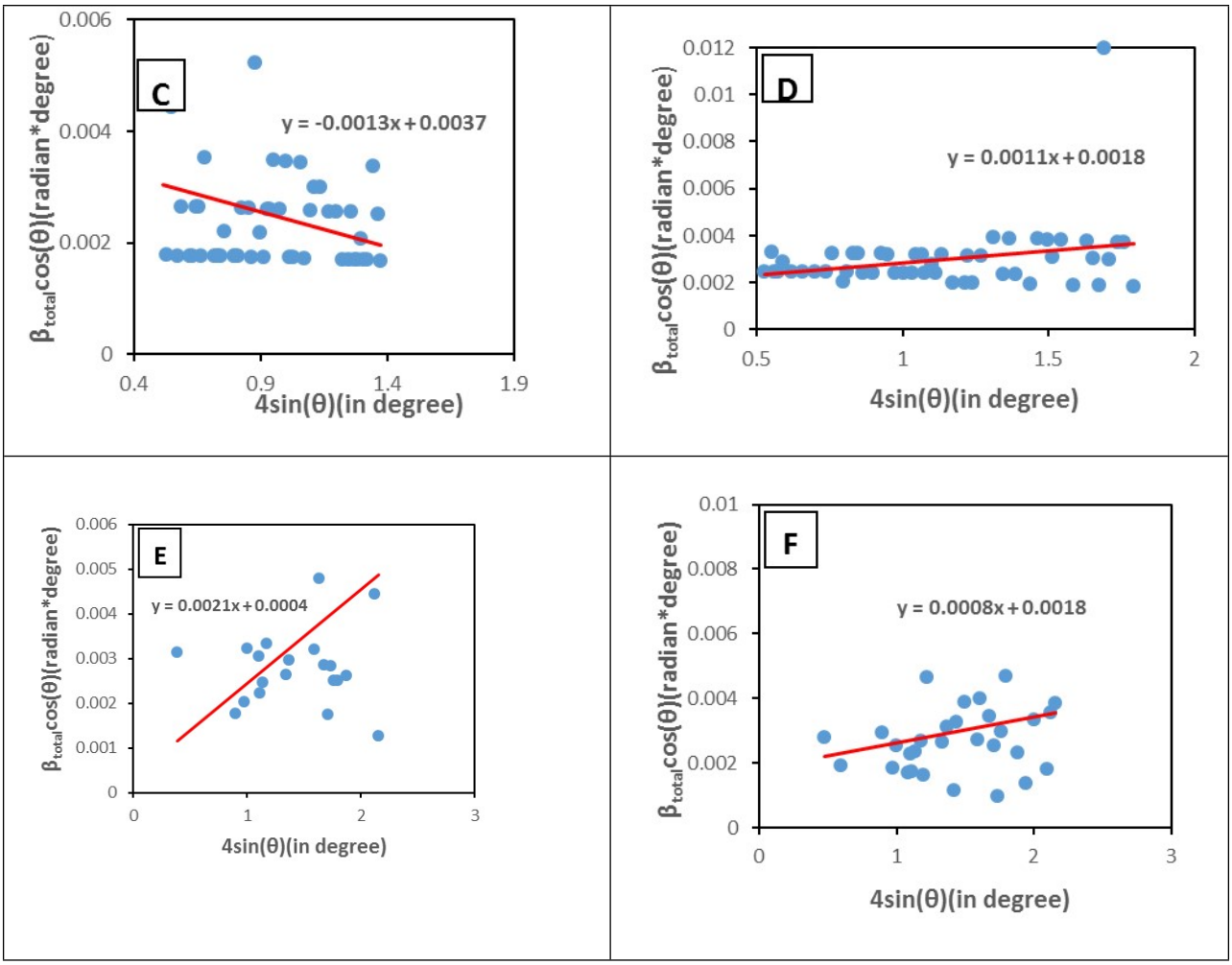

Figure S_3: Graphical representation of crystallite size for **(A)** HAp, (**B)** 0.32 Cu HAp, (**C)** 0.63 Cu HAp, (**D)** 1.25 Cu HAp, (**E)** 2.5 Cu HAp, (**F)** 5 Cu HAp using Williamson-Hall method.

Figure S_4: Optical band gap of synthesized HAp

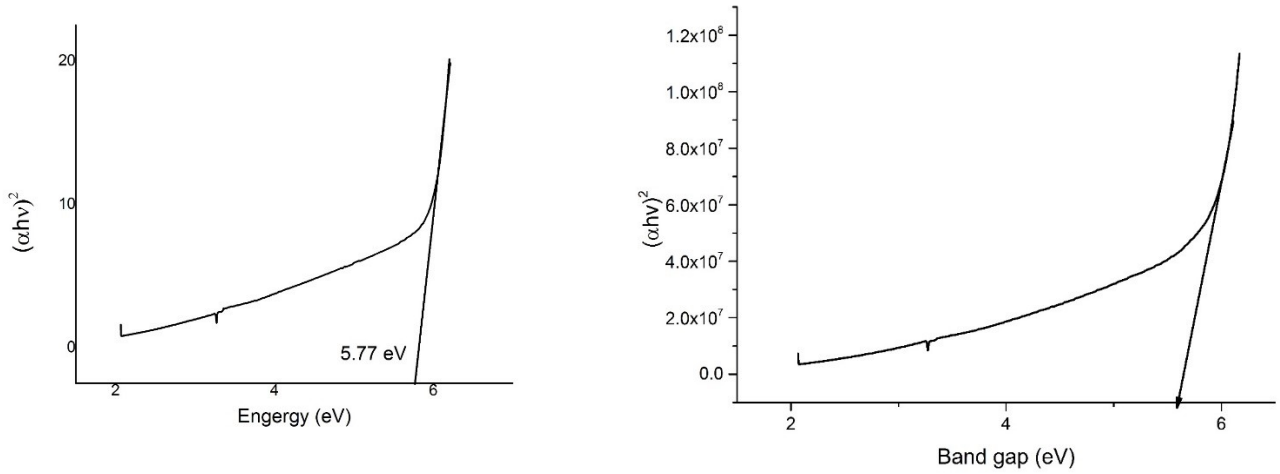

5.59 eV

Figure S_5: Optical band gap of synthesized 0.32Cu_Hap

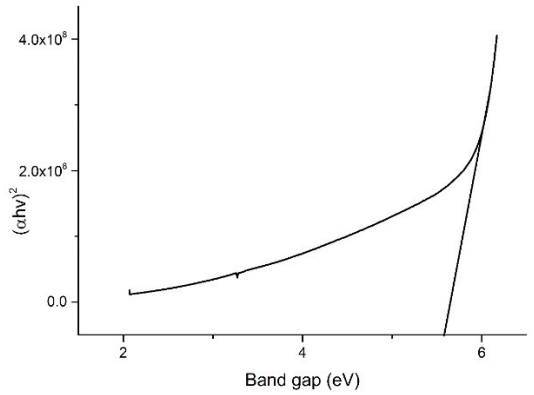

Figure S_6: Optical band gap of synthesized 0.63Cu_HAp

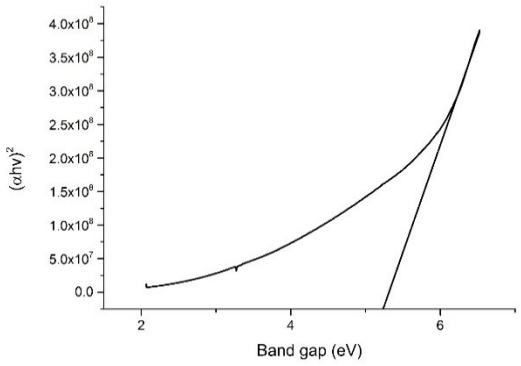

Figure S_7: Optical band gap of synthesized 1.25Cu_HAp

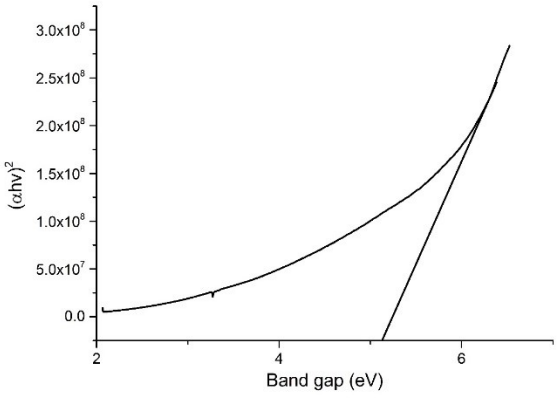

Figure S_8: Optical band gap of synthesized 2.5Cu_HAp

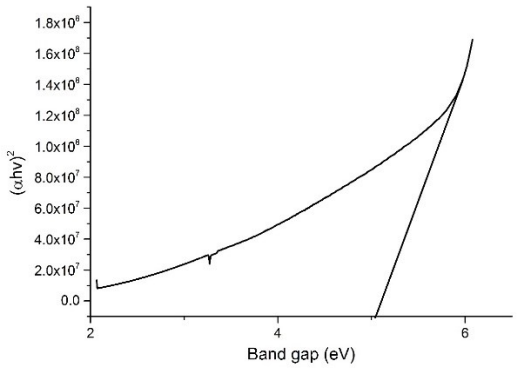

Figure S_9: Optical band gap of synthesized 5.0Cu_HAp

Adsorption study

3.2.Adsorption

The adsorption study was carried out to confine the dye molecule on the surface of the adsorbate or trap it on the bulk of the porous samples maintaining 180 min contact time, 0.2g adsorbent dose, 50 mL volume of 20 ppm solution. Dye molecules' diffusion to the active surface varied on the basis of the interaction of the adsorbate and adsorbent, and this interaction was controlled by changing the rotation (0-200 rpm) of the orbital shaker. The adsorbance percentages and capacity are presented in supplementary figure S_10, and the values were augmented with the rise of interaction (rpm) up to a certain limit, and after that, no significant variation was detected. This maximum limit of adsorption was achieved either by occupying the active surface for adsorbance or by filling up the pore volume of materials. Though all the prepared samples inherited excellent adsorption properties, the 0.63_Cu_HAp exhibited higher activity (adsorbance 93% and capacity 4.5 mg/g) than the others. The nature of the adsorption process was investigated employing adsorption isotherm estimation[4,5] with the assistance of two frequently used adsorption isotherms namely Langmuir and Freundlich adsorption isotherms. The removal/adsorbance percentage and adsorption capacity are significantly influenced by the initial concentration of Congo red dye and are revealed here in supplementary figure S_11. With the increment of initial concentration from 10 to 80 ppm, the removal percentage was considerably lessened but the removal capacity was linearly and sharply augmented. Any kind of adsorption process generates secondary waste materials which are also hazardous for the environment and additional disposal technique needs to be carried out. Thus, no further attention

was given to the adsorption process and we jumped to the photo catalysis technique.

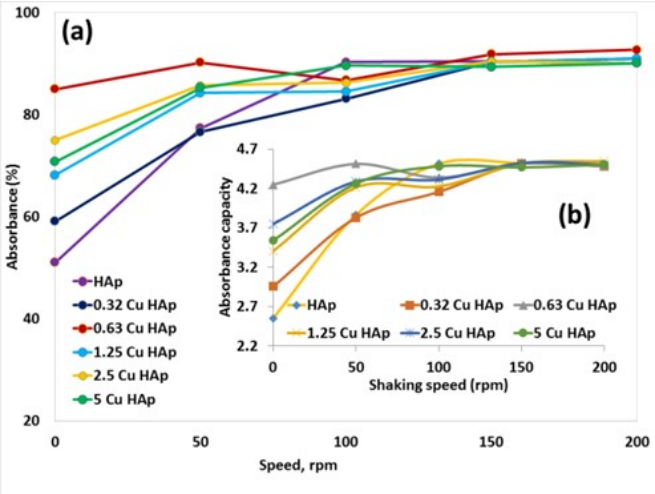

Figure S_10: Adsorption percentage and adsorption capacity of Congo red dye at different shaking speed [(a) absorbance (b) capacity]

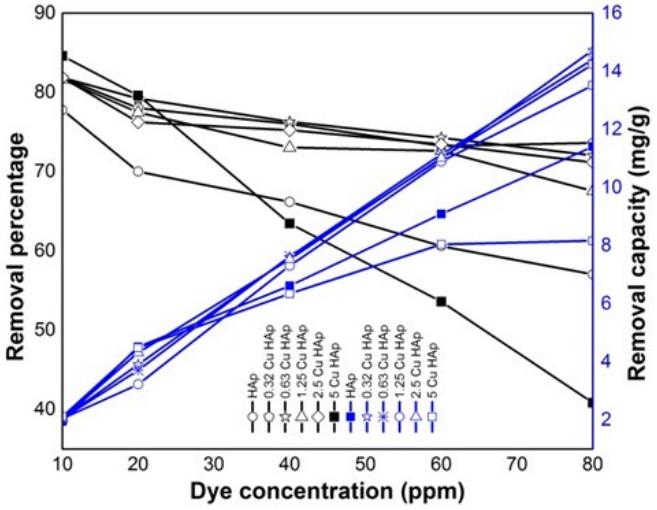

Figure S_11: Adsorption percentage and adsorption capacity of Congo red dye at a diverse initial concentration

Time optimization:

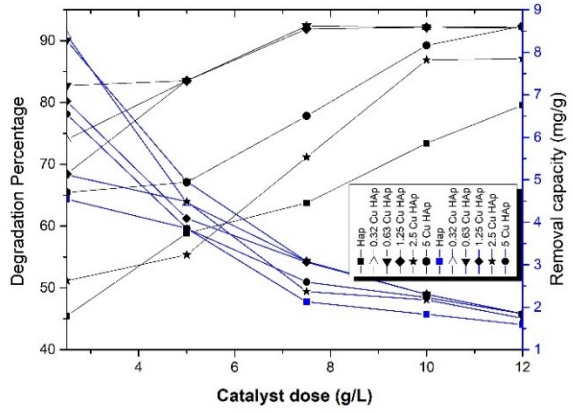

Figure S_12: Influence of various doses of photocatalyst with fixed 20 ppm Congo red dye

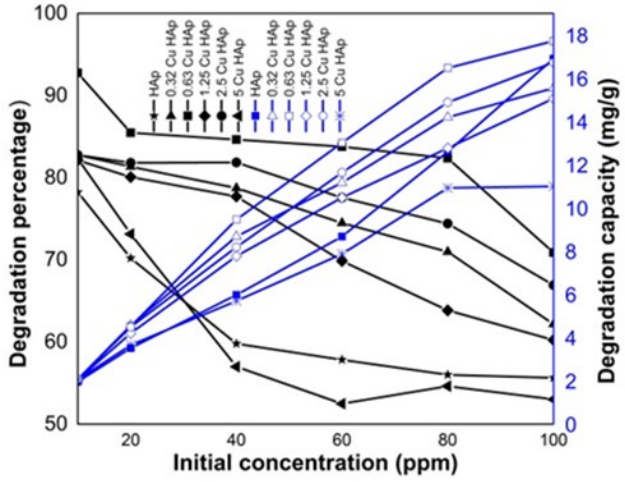

Figure S_13: Influence of different initial dye concentration for 0.2 g photocatalyst

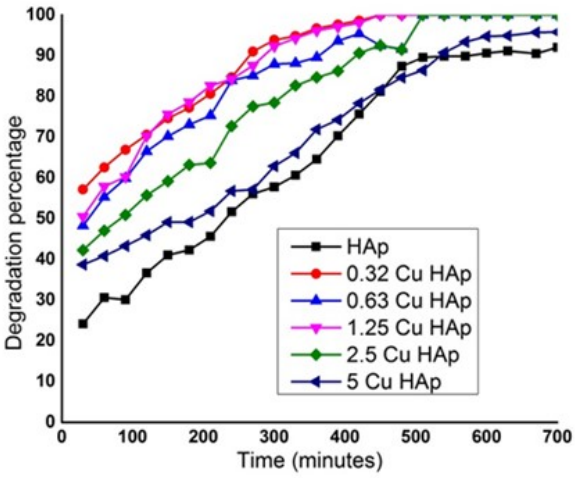

Figure S_14: Photodegradation percentages in terms of different time interval for catalyst dose of 0.1 g

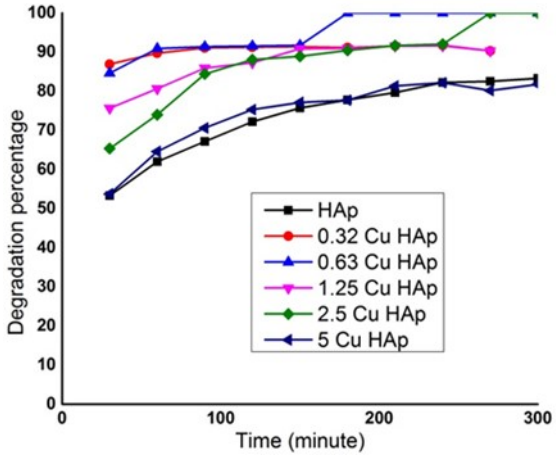

Figure S_15: Photodegradation percentages in terms of different time interval for catalyst dose of 0.2 g

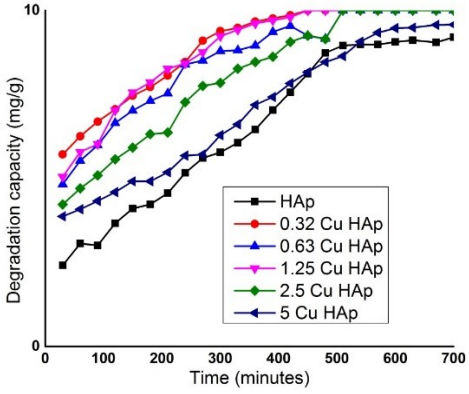

Figure S_16: Photo degradation capacity in terms of different time interval for catalyst dose 0.1 g

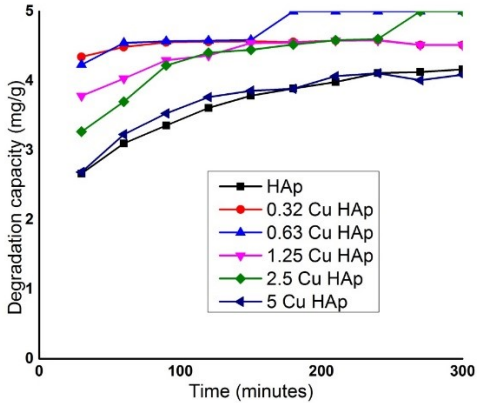

Figure S_17: Photo degradation capacity in terms of different time interval for catalyst dose 0.2 g

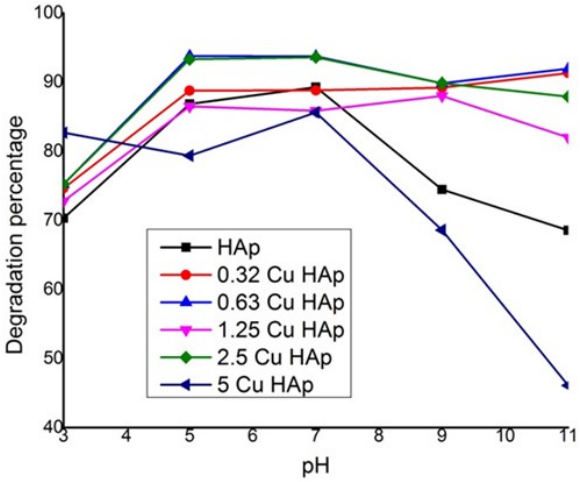

Figure S_18: Photochemical degradation percentage under different pH at 180 min, 50 mL of 20 ppm Congo red dye solution

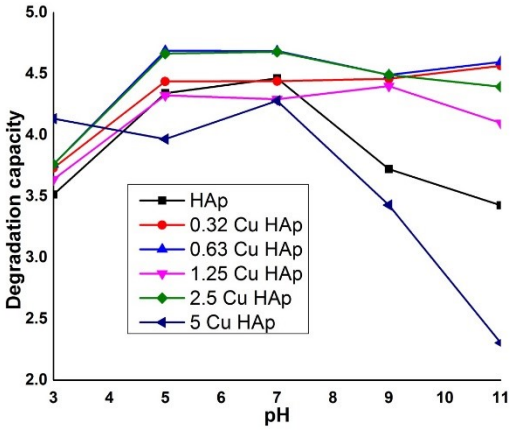

Figure S_19: Photochemical degradation capacity under different pH at 180 minutes, 50 ml of 20 ppm Congo red dye solution

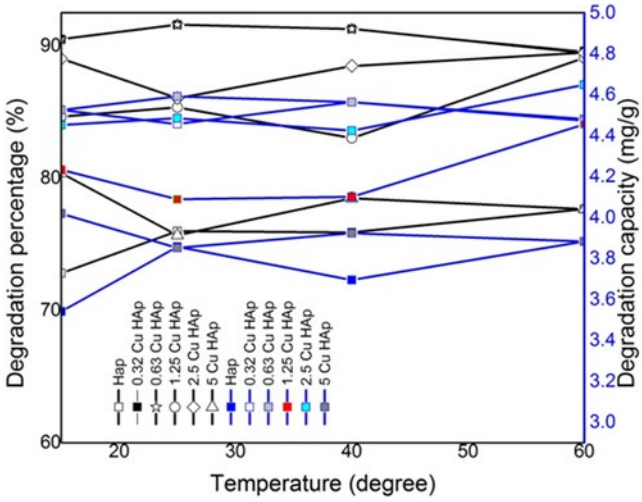

Figure 20: Influence of temperature on the photocatalytic efficiency of Congo red dye

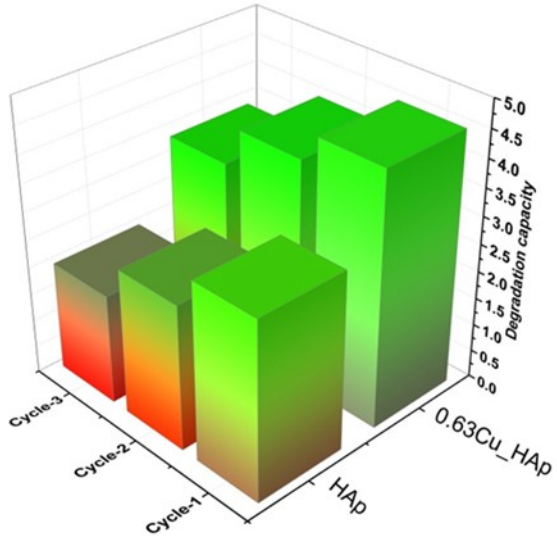

Figure S_21: Reuse property of pure HAp and 0.63Cu_HAp in terms of degradation capacity

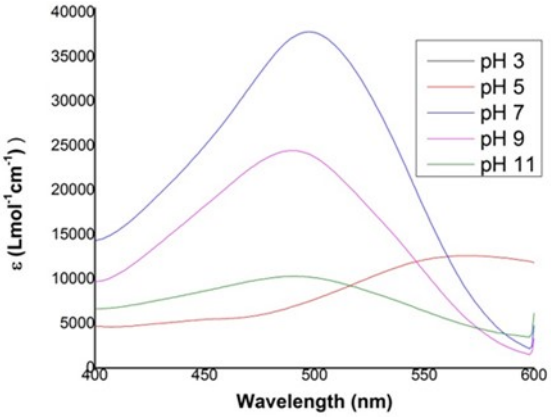

Figure S_22: Molar extinction coefficient of Congo red dye at various pH and fixed solution concentration 2.87×10^{-5} M (=20ppm)

Beer-Lambert law

The Beer-lambert law can be mathematically expressed as:

$$A = \varepsilon LC \quad (13)$$

Here, A= absorbance of radiation energy, C = concentration of the species, L = length of cuvette, and ε = proportionality constant. The proportionality constant is called molar absorptivity or extinction co-efficient when cuvette length is measured in centimeter and concentration is expressed in molarity. By rearranging equation (13) we get molar extinction co-efficient

$$\varepsilon = \frac{A}{LC} \quad (14)$$

For the Congo red of 20 ppm (2.87×10^{-5} M) and 1 cm cuvette length the molar extinction co-efficient was calculated at UV-vis spectral range.

Table S_1: Average calculated molar absorptivity

Sample ID	ε ($Lmol^{-1}cm^{-1}$)	Sample ID	ε ($Lmol^{-1}cm^{-1}$)
pH 3	8441.46	10 ppm	14668.29
pH 5	8441.46	20 ppm	22346.69
pH 7	22346.69	40 ppm	19459.76
pH 9	14668.29	60 ppm	9951.22
pH 11	7622.30	80 ppm	3667.189
-	-	100 ppm	1642.073

Photodegradation kinetics

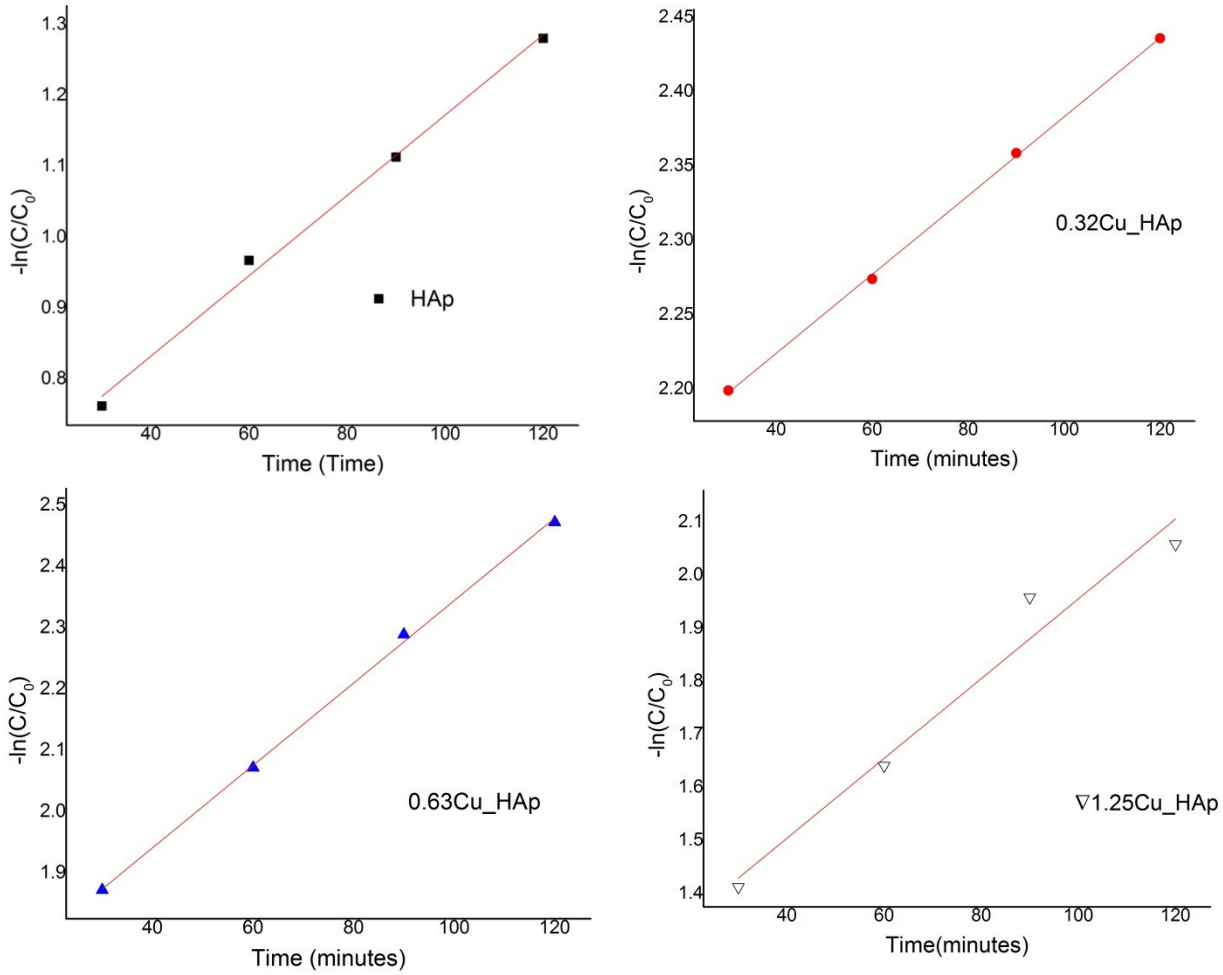

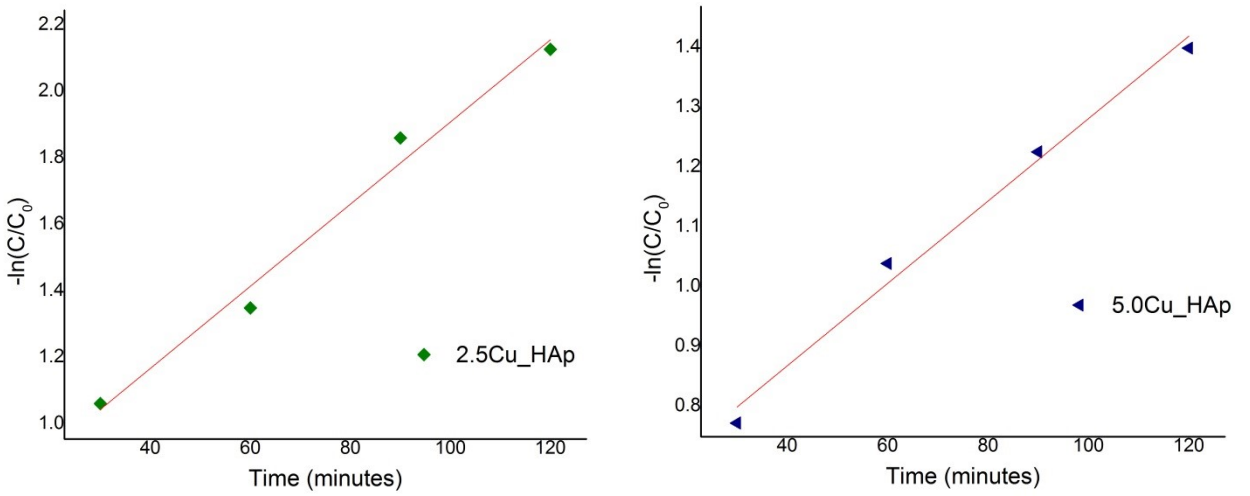

Figure S_23: Plot of –ln(C/C_0) against time (minutes) for various samples to calculate reaction rate constant for 0.2 g photo catalyst

Table S_2: Generated values of liner fit using Origin pro 9 software for different samples of 0.1 g photo catalyst dose

Column1	Intercept	Intercept2	Slope	Slope3	Statistics
	Value	Standard Error	Value	Standard Error	Adj. R-Square
HAp	0.21498	0.02225	0.00199	1.47E-04	0.9631
0.32 Cu HAp	0.685	0.03055	0.00467	2.02E-04	0.98708
0.63 Cu HAp	0.48505	0.06784	0.00494	4.48E-04	0.94516
1.25 Cu HAp	0.50547	0.0406	0.00474	2.68E-04	0.98496
2.5 Cu HAp	0.43187	0.04395	0.0032	2.90E-04	0.94525
5 Cu HAp	0.43285	0.01855	0.00153	1.22E-04	0.95695

Table S_3: Generated values of liner fit using Origin pro 9 software for different samples of 0.2 g photo catalyst dose

Column1	Intercept	Intercept2	Slope	Slope3	Statistics
	Value	Standard Error	Value	Standard Error	Adj. R-Square
HAp	0.60499	0.02277	0.00567	2.77E-04	0.99286
0.32 Cu HAp	2.11778	0.00345	0.00595	4.20E-05	0.99925
0.63 Cu HAp	1.67171	0.01235	0.00672	1.50E-04	0.9985
1.25 Cu HAp	1.20263	0.08113	0.00652	9.88E-04	0.95003
2.5 Cu HAp	0.67044	0.09113	0.00536	0.00111	0.97622
5 Cu HAp	0.59084	0.04246	0.005189	5.17E-04	0.98331

Freundlich adsorption isotherm

Heterogeneous surface with multilayer adsorption was estimated employing an empirical equation commonly known as Freundlich adsorption isotherm and the mathematical expression can be written as:

$$\frac{x}{m} = K_F C_e^{\frac{1}{n}} \quad (7)$$

Taking logarithm in both sides, equation (7) can be express as:

$$\log\left(\frac{x}{m}\right) = log(K_{F)} + log(C_e^{\frac{1}{n}}) \quad (8)$$

Or, $$\log\left(\frac{x}{m}\right) = log(K_{F)} + \frac{1}{n}log(C_e) \quad (9)$$

By rearranging equation (8), equation (9) can be generated

$$\log(q_e) = log(K_{F)} + \frac{1}{n}log(C_e) \quad (10)$$

Where, x= mass of adsorbate, x= mass of adsorbent, q_e= reaction capacity, $K_F =$ Frendlich constat denotes the adsorption capacity of adsorbent, n= another constant explains the adsorption process such as excellent adsorption (2 < n < 10), fairly complex adsoption (1 < n < 2) or difficult adsorption process(n < 1).

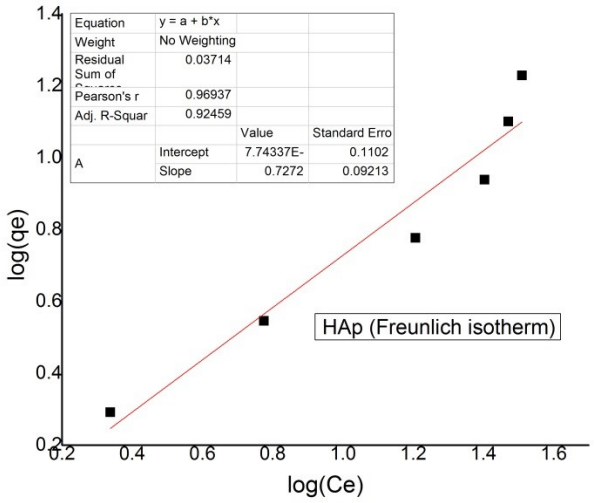

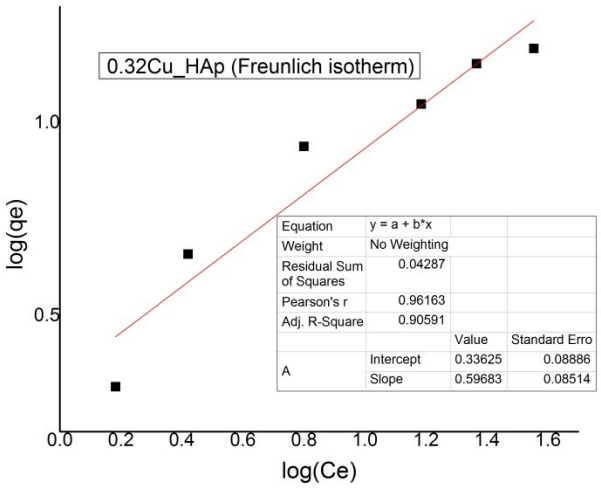

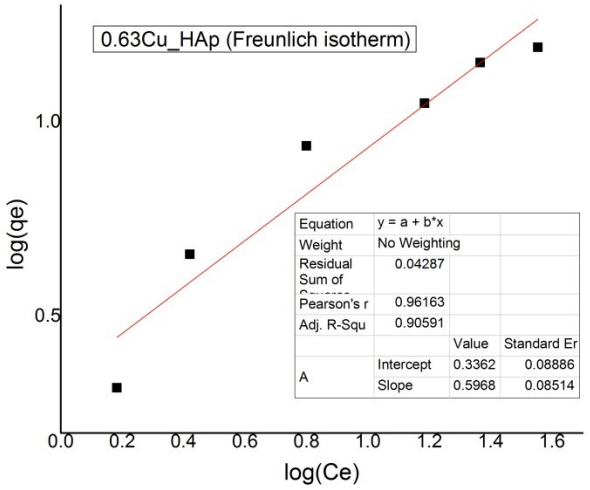

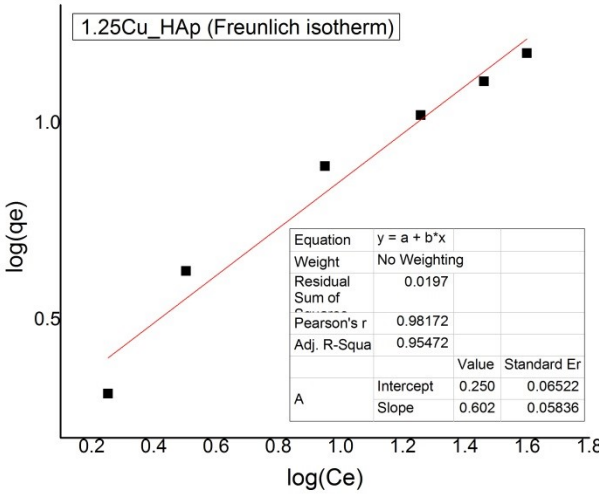

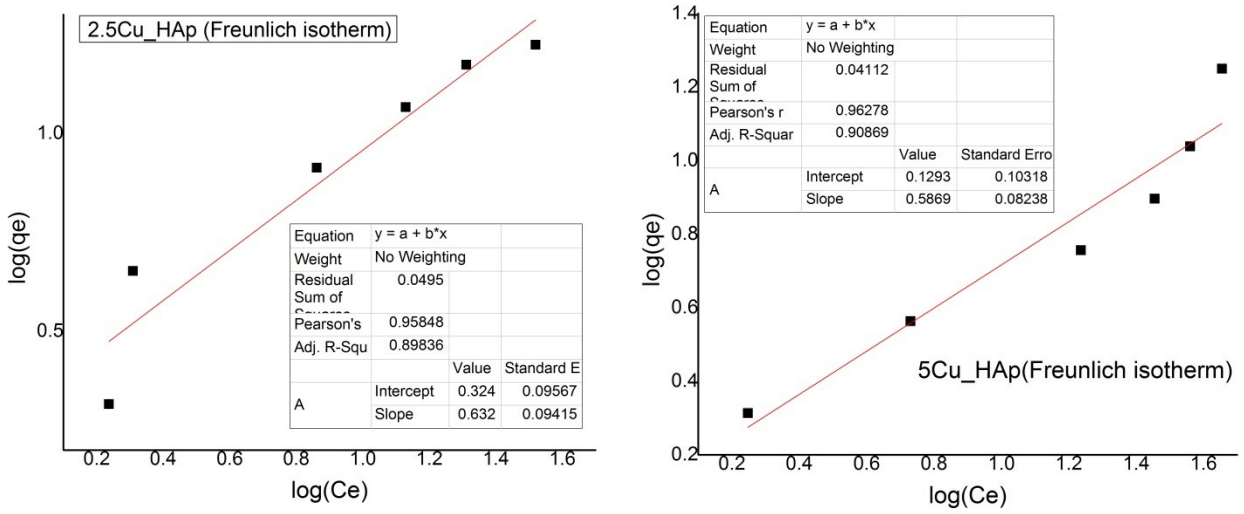

Figure S_24: Graphical presentation of Freundlich adsorption isotherm

S_3: Langmuir adsorption isotherm

The linear form of Langmuir adsorption isotherm:

$$\frac{C_e}{q_e} = \frac{1}{K_L q_{max}} + \frac{C_e}{q_{max}} \quad (11)$$

Where, $C_e =$ equilibrium concentration, $q_{e=}$ adsorption capacity at equilibrium condition, $q_{max=}$ maximum adsorption capacity, $K_{L=}$ Langmuir adsorption constant.

By plotting Ce/qe in y-axis and Ce in x-axis, straight line was built up and comparing slope and intercept with straight line (y=mx+c) K_L and q_{max} were calculated. Another dimensionless equilibrium parameter (R_L) was estimated from the Langmuir adsorption constant (K_L) and manifested as equation (12).

$$R_L = \frac{1}{1 + K_L C_{max}} \quad (12)$$

If, R_L = 1, isotherm is linear, if, 0 < R_L < 1 explains appropriate adsorption, R_L > 1 express disagreeable adsorption isothermal situation , R_L = 0 articulates irreversible adsorption.

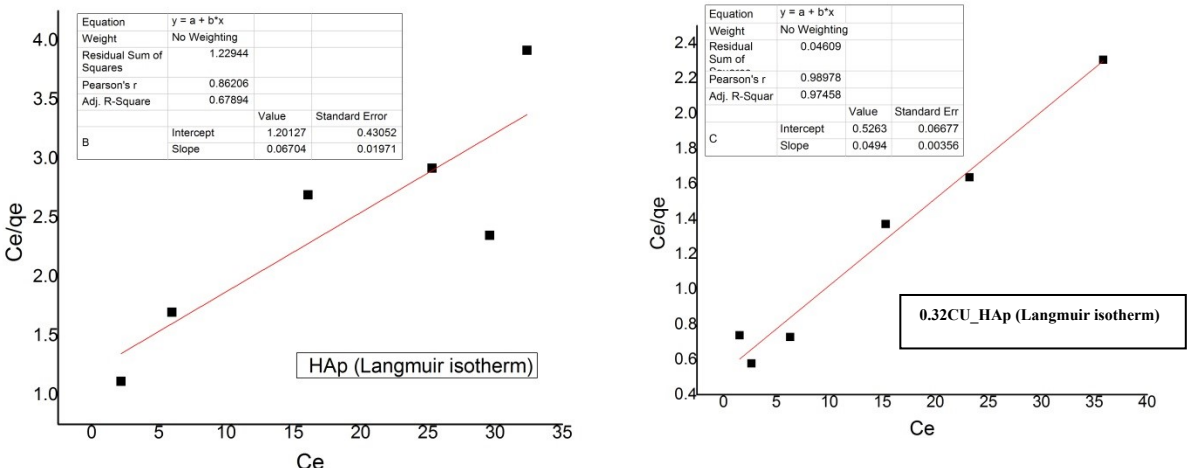

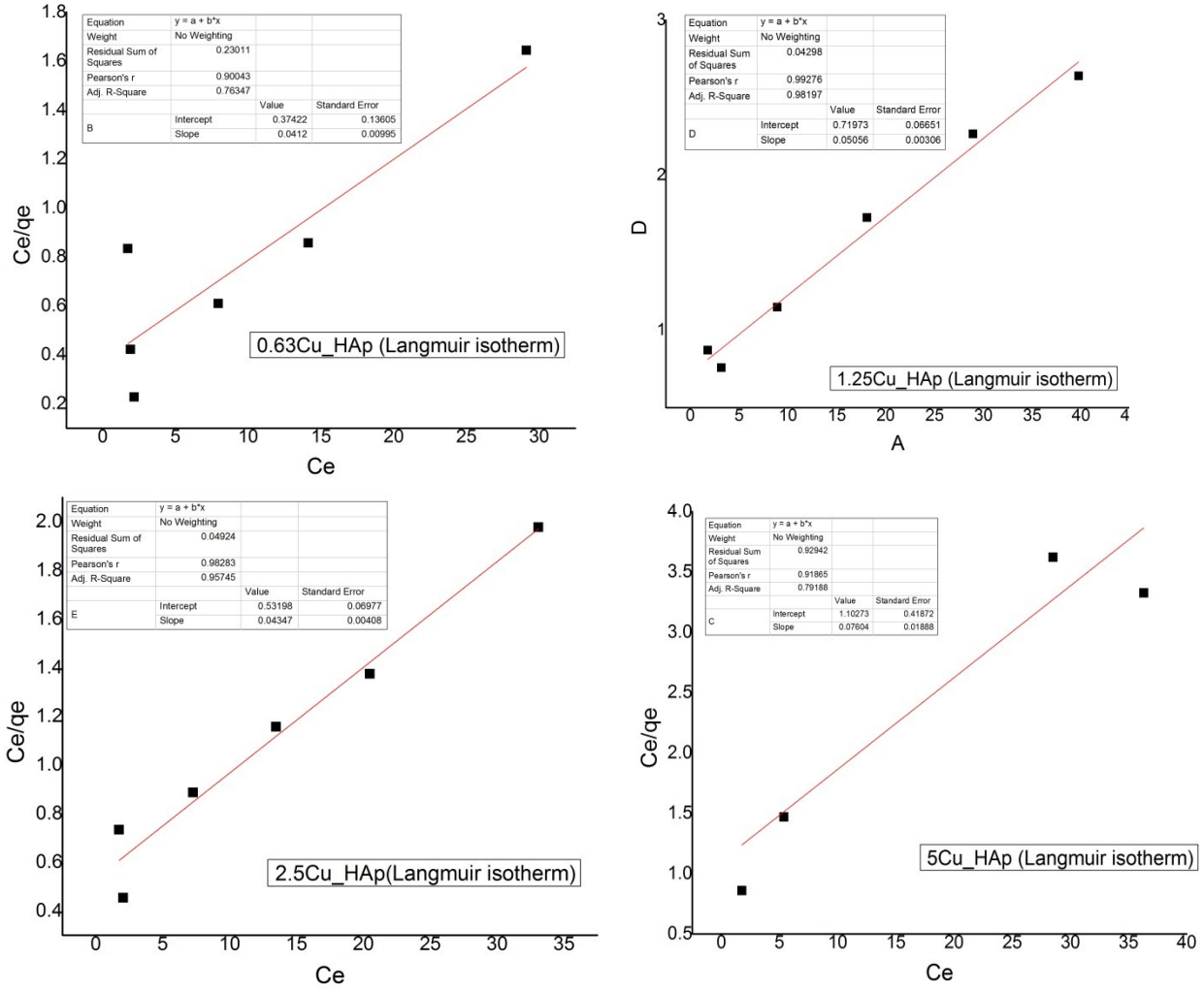

Figure S_25: Pictorial plot of Langmuir adsorption isotherm

Photo-degradation kinetics

If illumination is weakly absorbed by the system, HAp is well known weak photocatalyst, and then equation 18 can be simplified as first-order rate expression:

$$r = \left(-\frac{dC}{dt}\right)_{=} 2.303 E_{n,p,o}^{\ 0} \left(\frac{S}{V}\right) l\varepsilon\phi C \qquad (17)$$

If the rate constant (K_1) is taken as equation (17), the rate of first order reaction can be mathematically presented as equation (18).

$$K_{1=} 2.303 E_{n,p,o}^{\ 0} \left(\frac{S}{V}\right) l\varepsilon\phi \qquad (18)$$

$$\left(-\frac{dC}{dt}\right)_{=} K_1 C \qquad (19)$$

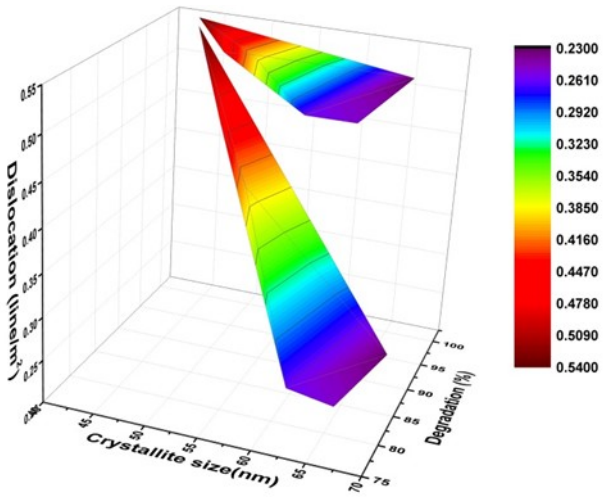

Figure S_26: Relationship among degradation percentage, crystallite size and dislocation density using Monshi-Scherrer method

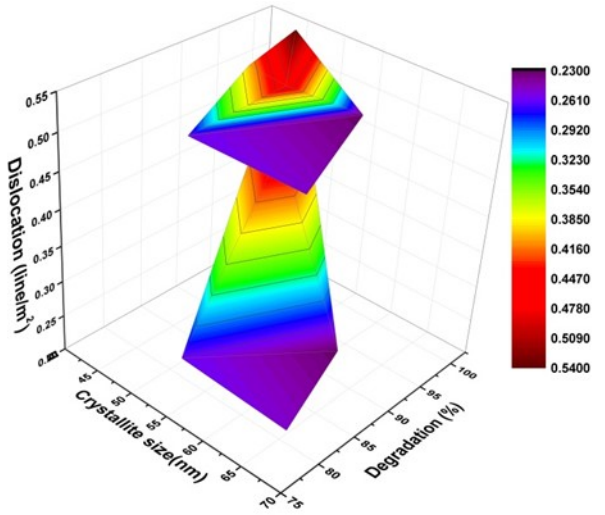

Figure S_27: Relationship among degradation percentage, crystallite size and dislocation density using William-Hall method

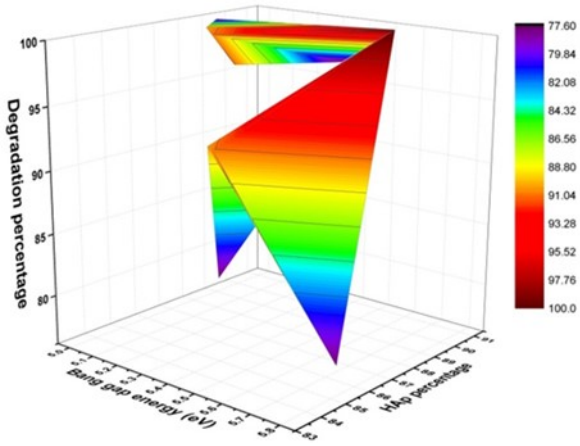

Figure S_28: Corelation among degradation percentage, percentage of HAp form and optical band gap energy

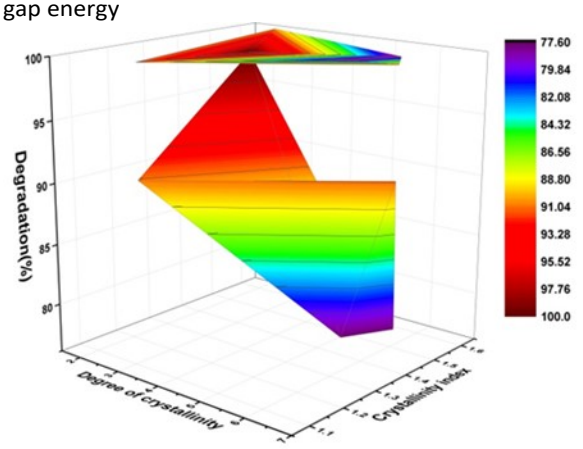

Figure S_29: Relationship among degradation percentage, degree of crystallinity and crystallinity index

References

(1) Khan, S. A.; Khan, S. B.; Asiri, A. M. Layered Double Hydroxide of Cd-Al/C for the Mineralization and de-Coloration of Dyes in Solar and Visible Light Exposure. *Scientific reports* **2016**, *6* (1), 1–15.

(2) Rahaman, M. S.; Hasnine, S. M. M.; Ahmed, T.; Sultana, S.; Bhuiyan, M. A. Q.; Manir, M. S.; Ullah, N.; Sen, S. K.; Hossain, M. N.; Hossain, M. S. Radiation Crosslinked Polyvinyl Alcohol/Polyvinyl Pyrrolidone/Acrylic Acid Hydrogels: Swelling, Crosslinking and Dye Adsorption Study. *Iranian Polymer Journal* **2021**, 1–16.

(3) Younis, S. A.; Motawea, E. A.; Moustafa, Y. M.; Lee, J.; Kim, K.-H. A Strategy for the Efficient Removal of Chlorophenols in Petrochemical Wastewater by Organophilic and Aminated Silica@ Alginate Microbeads: Taguchi Optimization and

Isotherm Modeling Based on Partition Coefficient. *Journal of hazardous materials* **2020**, *397*, 122792.
(4) Zheng, N.; Yin, L.; Su, M.; Liu, Z.; Tsang, D. C. W.; Chen, D. Synthesis of Shape and Structure-Dependent Hydroxyapatite Nanostructures as a Superior Adsorbent for Removal of U(VI). *Chemical Engineering Journal* **2020**, *384*, 123262. https://doi.org/10.1016/j.cej.2019.123262.
(5) Ali, J.; Wang, H.; Ifthikar, J.; Khan, A.; Wang, T.; Zhan, K.; Shahzad, A.; Chen, Z.; Chen, Z. Efficient, Stable and Selective Adsorption of Heavy Metals by Thio-Functionalized Layered Double Hydroxide in Diverse Types of Water. *Chemical Engineering Journal* **2018**, *332*, 387–397.